International Journal of Food Microbiology 238 (2016) 172–182

Contents lists available at ScienceDirect

International Journal of Food Microbiology

journal homepage: www.elsevier.com/locate/ijfoodmicro

Chemical, physical and morphological properties of bacterial biofilms affect survival of encased *Campylobacter jejuni* F38011 under aerobic stress

Jinsong Feng [a], Guillaume Lamour [b], Rui Xue [c], Mehr Negar Mirvakliki [d], Savvas G. Hatzikiriakos [d], Jie Xu [e], Hongbin Li [b], Shuo Wang [c], Xiaonan Lu [a,*]

[a] Food, Nutrition, and Health Program, Faculty of Land and Food Systems, The University of British Columbia, Vancouver, British Columbia V6T 1Z4, Canada
[b] Department of Chemistry, The University of British Columbia, Vancouver, British Columbia V6T 1Z1, Canada
[c] Key Laboratory of Food Nutrition and Safety, Ministry of Education of China, Tianjin University of Science and Technology, Tianjin 300457, China
[d] Department of Chemical and Biological Engineering, The University of British Columbia, Vancouver, British Columbia V6T 1Z3, Canada
[e] Department of Mechanical and Industrial Engineering, University of Illinois at Chicago, Chicago, IL 60607, United States

ARTICLE INFO

Article history:
Received 25 January 2016
Received in revised form 22 June 2016
Accepted 11 September 2016
Available online 13 September 2016

Keywords:
Raman spectroscopy
Atomic force microscopy
Confocal laser scanning microscopy
Contact angle measurement

ABSTRACT

Campylobacter jejuni is a microaerophilic pathogen and leading cause of human gastroenteritis. The presence of *C. jejuni* encased in biofilms found in meat and poultry processing facilities may be the major strategy for its survival and dissemination in aerobic environment. In this study, *Staphylococcus aureus*, *Salmonella enterica*, or *Pseudomonas aeruginosa* was mixed with *C. jejuni* F38011 as a culture to form dual-species biofilms. After 4 days' exposure to aerobic stress, no viable *C. jejuni* cells could be detected from mono-species *C. jejuni* biofilm. In contrast, at least 4.7 log CFU/cm^2 of viable *C. jejuni* cells existed in some dual-species biofilms. To elucidate the mechanism of protection mode, chemical, physical and morphological features of biofilms were characterized. Dual-species biofilms contained a higher level of extracellular polymeric substances with a more diversified chemical composition, especially for polysaccharides and proteins, than mono-species *C. jejuni* biofilm. Structure of dual-species biofilms was more compact and their surface was >8 times smoother than mono-species *C. jejuni* biofilm, as indicated by atomic force microscopy. Under desiccation stress, water content of dual-species biofilms decreased slowly and remained at higher levels for a longer time than mono-species *C. jejuni* biofilm. The surface of all biofilms was hydrophilic, but total surface energy of dual-species biofilms (ranging from 52.5 to 56.2 mJ/m^2) was lower than that of mono-species *C. jejuni* biofilm, leading to more resistance to wetting by polar liquids. This knowledge can aid in developing intervention strategies to decrease the survival and dispersal of *C. jejuni* into foods or environment.

1. Introduction

Campylobacter jejuni is a Gram-negative, microaerophilic bacterium and is one of the leading causes of foodborne gastrointestinal diseases worldwide. *Campylobacter* infection causes an acute gastroenteritis characterized by inflammation, abdominal pain, fever and diarrhea (Young et al., 2007). Previous reports indicated that *C. jejuni* infection cases in Canada outnumbered reported cases of *Escherichia*, *Listeria*, *Shigella* and *Salmonella* infections combined (Kalmokoff et al., 2006). The paradox associated with *C. jejuni* is that this bacterium is prevalent in the environment and difficult to eliminate from the food chain; however, as a microaerophile, *C. jejuni* is sensitive to aerobic stress and does not multiply in the aerobic environment. Studies have confirmed that bacteria shed from biofilms could continue to contaminate foods, potentially leading to food poisoning (Donlan and Costerton, 2002; Kumar and Anand, 1998). Under this condition, *C. jejuni* may survive within a biofilm microenvironment and further lead to food contamination (Ica et al., 2012), even though there remain controversies about how *C. jejuni* can resist environmental stress (*e.g.*, temperature fluctuation, aerobic, or shear stress) and form biofilms alone (Teh et al., 2014). In the natural environment, bacterial cells mainly reside in a multispecies culture. According to the previous reports, *C. jejuni* biofilms are present in the gastrointestinal tract of poultry, in water supply and plumbing systems in animal husbandry facilities and food processing plants (Hermans et al., 2011; Newell and Fearnley, 2003; Siringan et al., 2011; Trachoo et al., 2002) along with other foodborne pathogens including *Staphylococcus aureus*, *Salmonella enterica*, and *Pseudomonas aeruginosa*. The biofilms formed by these microorganisms are believed to provide protection to *C. jejuni* against antimicrobial treatments and aerobic stress (Ica et al., 2012; Joshua et al., 2006).

* Corresponding author.
E-mail address: xiaonan.lu@ubc.ca (X. Lu).

http://dx.doi.org/10.1016/j.ijfoodmicro.2016.09.008
0168-1605/

Biofilms have a complex chemical composition. In the particulate fraction of a biofilm, up to 90% is composed by extracellular polymeric substances (EPS) including polysaccharides, proteins, nucleic acids, lipids, and humic-like substances. Specific chemical components of a biofilm may contribute to its resistance to exogenous stress. For example, hydrophilic polysaccharides and proteins in EPS can hold water and keep entrained microbial cells hydrated limiting the impact of desiccation stress (Roberson and Firestone, 1992; Tamaru et al., 2005). Enzymes within biofilms could inactivate stress inducers and neutralize these in a biofilm microenvironment (Davies, 2003). Unfortunately, it has been difficult to characterize the chemical profiles of biofilms because common methods, such as crystal violet (Reeser et al., 2007) and Congo red staining (Reuter et al., 2010), are destructive and can only be used to evaluate the biofilm formation level. Innovative spectroscopic methods, particularly Raman spectroscopy coupled with confocal technique can provide *in situ* and nondestructive determination of the chemical composition of bacterial biofilms and changes in the composition of biofilms in response to various forms of stress (Ivleva et al., 2008; Ivleva et al., 2010; Lu et al., 2012a).

Besides chemical composition, morphological properties of bacterial biofilms are also important in determining their resistance to the environmental stress. Joshua and coauthors compared biofilms produced by wild-type and mutant *C. jejuni* strains using scanning electron microscopy (SEM) (Joshua et al., 2006). Reuter and coworkers evaluated surface adhesion and microstructure of *C. jejuni* mono-species biofilm formed under microaerobic and aerobic environment using light microscopy after staining (Reuter et al., 2010). Both studies confirmed that the assemblage structure of biofilms were associated with the survival of encased sessile cells under environmental stress. Due to the destructive sample preparation process (*e.g.*, chemical fixation for SEM, staining for light microscopy), artifacts may be introduced that affect accurate characterization of biofilms. Atomic force microscopy (AFM) offers an alternative characterization methodology. By recording interaction signals between the probing tip and biofilm surface, AFM can generate high-resolution topographic images that accurately reflect the structural details of morphological information of a biofilm in a nano-scale without sample preparation (Ivanov et al., 2011; La Storia et al., 2011; Lim et al., 2011; Scheuring and Dufrêne, 2010).

Physical properties of biofilms, such as surface wettability (hydrophobicity/hydrophilicity), surface roughness, surface free energy, and water holding capability, play a role in the response of bacterial biofilms to a variety of stresses, such as desiccation and shear stress (Bove et al., 2012; Ng and Kidd, 2013). Wettability is related to the surface area of biofilm that could contact water while a high water holding capability maintains a high relative humidity in biofilms, both of which are important to protect encased cells from desiccation (Allison et al., 1990). Surface roughness predicts the susceptibility of biofilms to shear force, thus the smoother the biofilm surface the less it is influenced by mechanical shearing forces (Beech et al., 2002; Li and Logan, 2004).

Few studies have been conducted to investigate the effect of mixed bacterial culture on *C. jejuni*-containing biofilms and the susceptibility of *C. jejuni* cells in these multispecies biofilms. Therefore, the aim of this study is to characterize chemical, physical and morphological properties of dual-species *C. jejuni*-containing biofilms and correlate these to the stress resistance of encased *C. jejuni* cells compared to that of mono-species *C. jejuni* biofilm. The knowledge will be important to further understand the ecology of *C. jejuni* and its survival in the environment and subsequently develop innovative mitigation strategies to more successfully eliminate biofilms and reduce public health risk associated with this microbe.

2. Materials and methods

2.1. Bacterial strains and cultivation

C. jejuni F38011 (human clinical isolate), *Staphylococcus aureus* (a clinical isolate used in our previous study) (Lu et al., 2013), *Salmonella enterica* serovar Enteritidis FDA 3512H, and *Pseudomonas aeruginosa* PAO1 were used in this study. *C. jejuni* strain was stored at −80 °C in Mueller-Hinton (MH) broth (BD Difco) containing 12% glycerol and 75% defibrinated sheep blood. Routine cultivation was conducted either on *Campylobacter* agar (OXOID) supplemented with 5% defibrinated sheep blood or in MH broth with constant shaking at 37 °C under microaerobic conditions (85% N_2, 10% CO_2, 5% O_2). *S. aureus*, *S. enterica*, and *P. aeruginosa* were individually cultivated overnight in 5 ml tryptic soy broth (TSB) (BD Difco) at 37 °C to achieve a concentration of *ca.* 9 log CFU/ml.

2.2. Biofilm cultivation

One milliliter of overnight bacterial culture was centrifuged at 8000 × *g* for 10 min at 22 °C. The supernatant was discarded and the bacterial pellets were washed twice and resuspended in sterile phosphate buffered saline (PBS) (pH = 7.0). The resuspended culture was then diluted to ~10^7 CFU/ml. For dual-species biofilm formation, the mixed culture of *C. jejuni* F38011 was generated by addition of a second bacterial strain listed above on the basis of the same volume and concentration. Biofilms were cultivated at both solid-air interface and solid-liquid interface. Nitrocellulose membrane (0.45 mm pore size, 47 mm diameter; Sartorius Stedim-type filters) was used as substrate for biofilm formation at solid-air interface, as described elsewhere (Lu et al., 2012a, 2012b). *C. jejuni* monoculture or mixed culture (100 μl) was deposited onto the surface of a sterile nitrocellulose membrane with a surface area of ~3 × 3 cm^2, which was placed onto an agar plate supplemented with 5% defibrinated sheep blood and incubated under microaerobic environment at 37 °C. The membrane was aseptically transferred to a fresh agar plate every 24 h for up to 72 h. To cultivate biofilms at liquid-solid interface, 0.2 ml of *C. jejuni* monoculture or mixed culture was added into each well of sterile 96-well polystyrene plate. The plate was incubated under microaerobic environment at 37 °C for up to 72 h.

2.3. Survival of *C. jejuni* F38011 and co-cultured bacterial cells in biofilms under aerobic stress

C. jejuni and co-cultured bacterial cell survival in mono-species and dual-species biofilms under aerobic stress were determined by selective agar. Briefly, mature biofilms (cultivated under microaerobic condition for 72 h) formed on nitrocellulose membrane were placed under aerobic environment at 22 °C for up to 5 days. Every 24 h, biofilms were detached from nitrocellulose membrane using 0.1% trypsin solution (20 ml) for incubation at 22 °C for 20 min. This treatment did not affect bacterial cell viability (data not shown). Following detachment, the bacterial suspension was serially diluted and spread onto selective agar plate. Campy Cefex agar is used for enumeration of viable *C. jejuni* cells (Neal-McKinney et al., 2012). Campy-Cefex agar contains 43 g/l Brucella agar, 0.5 g/l ferrous sulfate, 0.2 g/l sodium bisulfite, 0.5 g/l sodium pyruvate, 33 mg/l cefoperazone, and 0.2 g/l cycloheximide, with a supplement of 5% defibrinated sheep blood (Oyarzabal et al., 2005). Mannitol salt agar (BD BBL) is used for the enumeration of viable *S. aureus* cells. Xylose lysine deoxycholate (XLD) agar (BD Difco) is used for enumeration of viable *S. enterica* and *P. aeruginosa* cells. The selective agar for *C. jejuni* was placed under microaerobic environment at 37 °C, while selective agars for co-cultured bacterial strains were placed under aerobic environment at 37 °C.

2.4. Confocal laser scanning microscopy (CLSM)

The survival state of *C. jejuni* cells within a biofilm was further confirmed using CLSM. The SYTO 9 dye (with a green color for live cells) and propidium iodide dye (with a red color for non-viable cells) were

diluted according to the manufacturer's instructions and then mixed in equal volume proportions. After exposure to aerobic environment for 4 days, nitrocellulose membrane with a developed biofilm was transferred from an agar plate to a sterile petri dish with 2 ml of the mixed dye solution, followed by incubation at 22 °C for 30 min in the absence of light. The unbound dye was rinsed off of the nitrocellulose membrane with PBS (pH 7.0) and images of stained biofilms were collected using a confocal microscopy (FV3000, Olympus, Tokyo, Japan). The wavelengths of excitation laser were set at 488 nm and 543 nm for green channel and red channel, respectively. Images were collected using a 40.0 × 1.0 oil immersion objective lens at a scan speed of 400 Hz.

2.5. Crystal violet biofilm assay

Crystal violet staining was applied to quantify biofilm formation at the liquid-solid interface. After 72 h cultivation, a 96-well plate was washed with sterile deionized water and dried at 37 °C for 5 min. Then, 0.2 ml of 0.5% (w/v) crystal violet solution was added into each well of 96-well plate, and the plate was incubated at 22 °C for 10 min. Unbound crystal violet was washed off with sterile deionized water, and the plate was dried at 22 °C for another 5 min. Bound crystal violet was dissolved in 0.2 ml of 95% ethanol (v/v) for 10 min. Released crystal violet suspension was measured using a microplate reader at 595 nm (SpectraMax M2, Molecular Devices, Sunnyvale, USA). Broth without bacterial inoculation was stained using the same method as control and subtracted for background correction.

2.6. C. jejuni share (CJS) index in biofilm formation

CJS index is used to semi-quantify the contribution of encased *C. jejuni* cells to the formation of dual-species biofilm compared to the formation of mono-species biofilm. CJS index is calculated as previously described (Naves et al., 2008) with modifications:

$$\mathrm{CJS} = \frac{\mathrm{AB}-\mathrm{NCS}}{\mathrm{C}} \Big/ \frac{\mathrm{AC}-\mathrm{CS}}{\mathrm{CO}},$$

in which AB is the optical density of crystal violet stained dual-species biofilms, AC is the optical density of crystal violet stained mono-species *C. jejuni* biofilm, NCS is the optical density of crystal violet stained mono-species non-*C. jejuni* biofilm (*i.e. S. aureus*, *S. enterica*, and *P. aeruginosa*), CS is the optical density of crystal violet staining without inoculation, C is the viable *C. jejuni* cell counts in the mature dual-species biofilm, CO is the viable *C. jejuni* cell counts in the mature mono-species *C. jejuni* biofilm.

2.7. Confocal micro-Raman spectroscopy

This photonic system includes a Raman spectrometer (Renishaw, Gloucestershire, United Kingdom), a Leica microscope (Leica Biosystems, Wetzlar, Germany) and a diode near-infrared (λ = 785 nm) laser (Renishaw, Gloucestershire, United Kingdom). The spectrometer has an entrance aperture of 50 μm and a focal length of 300 mm and is equipped with 1200-line/mm grating. Raman scattering signals were collected and dispersed by a diffraction grating and finally recorded as a Raman spectrum by a 576-by-384-pixel charge-coupled-device (CCD) array detector, with the size of each pixel 22 by 22 μm. Mono-species and dual-species *C. jejuni* biofilms formed at solid-air interface were directly transferred onto the microscope stage, which was focused under the collection assembly, and spectra were collected using a 50× objective (numerical aperture [NA] = 0.75, working distance [WD] = 0.37 mm) with a wavenumber range of 1800–400 cm^{-1}. The spectral collection was conducted over a total of 60 s (exposure time) at eight different locations for each biofilm with ~25 mW of incident laser power. Exposure to laser illumination during Raman spectral collection did not cause damage or variations in chemical components of biofilm samples (data not shown).

2.8. Raman spectral processing and multivariate analysis

The polynomial background fit combined with baseline subtraction was carried out to remove fluorescence background derived from biofilms. Spectral binning (2 cm^{-1}) and smoothing (9-point Savitzky-Golay algorithm) were then applied (Feng et al., 2014).

Due to the potential minor differences among Raman spectra derived from biological variation among biofilm samples, a second derivative transformation algorithm was applied to amplify the minor spectral variations and separate out overlapping bands (Lu et al., 2011a, 2011b). Unsupervised PCA models were constructed to quantify the variation among different biofilm samples. *Mahalanobis* distances in the PCA models were calculated to evaluate the variation among different biofilms (Lu et al., 2013).

2.9. Atomic force microscopy

The variations in morphological properties between mono-species and dual-species *C. jejuni* biofilms formed at solid-air interface were determined using a Cypher atomic force microscope (Asylum Research, Santa Barbara, U.S.A.) and TR400PB tip cantilevers from Olympus (Tokyo, Japan; nominal spring constant: k = 0.02 N/m). Topographic images were collected in contact mode in ambient air. The nitrocellulose membrane with a mature biofilm grown (cultivated under microaerobic condition at 37 °C for 72 h) was transferred from agar plate onto AFM specimen disc (15 mm diameter, Ted Pella, Redding, CA). After drying in biological safety cabinet at 22 °C at <30% relative humidity for 30 min without air blowing, the specimen disc coated with biofilm was put into an enclosed sample chamber at 22 °C at <60% relative humidity. Topographic images were collected at 5 random locations on the biofilm surface with a surface area of 8 μm × 8 μm at scan frequency of 1 Hz. The AFM system was operated using Igor Pro 6.31 software (Wavemetrics Inc., Lake Oswego, U.S.A.) and the AFM images were analyzed off-line using WSxM 5.0 software (Nanotec Electronica S.L., Madrid, Spain). Surface root-mean-square (RMS) roughness of biofilms was calculated using height images with a surface area of 8 μm × 8 μm.

2.10. Contact angle measurement

The wettability (hydrophobic/hydrophilic) of biofilm surfaces were determined by contact angle measurement using a sessile drop method (Lamour et al., 2010; Syamaladevi et al., 2013). In this study, sterile deionized water, formamide and diiodomethane were used as reference liquids. Briefly, mature biofilms (cultivated under microaerobic condition for 72 h) formed at the solid-air interface were dried at 22 °C for 30 min before contact angle measurement. Then, 1 μl liquid droplet was deposited onto the biofilm surface and allowed to settle for 5 s. A high-resolution digital camera (D90, Nikon, Tokyo, Japan) was used to capture profile images of contact angles at the equilibrium under a light source. Contact angle (θ) was collected at three random locations for each sample and experiment was conducted in triplicate.

Images were analyzed by software FTA32 Version 2.0 (First Ten Ångstroms, Portsmouth, U.S.A.), as described by Mirvakili and Beyenal (Beyenal et al., 2004; Mirvakili et al., 2013). Biofilm wettability was estimated by contact angle formed by deionized water. Biofilm surface free energy properties [*i.e.*, total surface energy (γ_S), Lewis acid-base component (γ_S^{AB}), Lifshitz-van der Waals (γ_S^{LW}), electron-donor (γ_S^-) and electron acceptor (γ_S^+)] were calculated according to Young-

Dupré equation and van Oss approach (Briandet et al., 2001; van Oss, 2002) as follows:

$$\cos\theta = -1 + {}^{2}\sqrt{\left(\gamma_S^{LW}\gamma_L^{LW}\right)}\Big/_{\gamma_L} + {}^{2}\sqrt{\left(\gamma_S^{+}\gamma_L^{-}\right)}\Big/_{\gamma_L} + {}^{2}\sqrt{\left(\gamma_S^{-}\gamma_L^{+}\right)}\Big/_{\gamma_L}$$

$$\gamma_S^{AB} = 2\sqrt{\left(\gamma_S^{+}\gamma_S^{-}\right)}$$

$$\gamma_S = \gamma_S^{AB} + \gamma_S^{LW}$$

The surface energy properties of reference liquids (*i.e.*, water, formamide and diiodomethane) are listed in Supplementary materials (Table S2).

2.11. Biofilm water retention assays

Attenuated total reflectance-Fourier transform infrared (FT-IR) spectroscopy was applied to determine water holding capability of mono-species and dual-species *C. jejuni* biofilms formed at solid-air interface. After 72 h cultivation, nitrocellulose membranes with developed biofilms were removed from agar plates and immediately mounted onto the crystal cell of Spectrum 100 FT-IR spectrometer (PerkinElmer, Norwalk, U.S.A.). FT-IR spectra of each biofilm were recorded at 22 °C at intervals of 5 min until no changes in spectral features. Previous work has shown that spectral features of the nitrocellulose membrane did not affect FT-IR spectral features of biofilms since the penetration distance of the evanescent wave derived from mid-IR is less than the thickness of biofilm (Lu et al., 2012a).

2.12. Statistical analysis

All the experiments were conducted in at least three replicate trials. Results were reported as the averages of replicates ± the standard deviation with significance ($P < 0.05$) by one-way analysis of variance (ANOVA).

3. Results

3.1. Survival of C. jejuni F38011 and co-cultured bacterial cells in developed biofilms under aerobic stress

In mature biofilms, the presence of *S. enterica* and *S. aureus* in dual-species biofilms did not affect the growth of *C. jejuni*, and the culturable *C. jejuni* cell counts in *C. jejuni-S. enterica* and *C. jejuni-S. aureus* biofilms were not significantly different ($P > 0.05$) compared to the mono-species *C. jejuni* biofilm during biofilm development. However, dual-species biofilm containing *P. aeruginosa* had a significantly lower ($P < 0.05$) number of culturable *C. jejuni* cells, about two orders of magnitude lower compared to the mono-species *C. jejuni* biofilm (Table 1). On the other hand, the presence of *C. jejuni* in dual-species biofilms did not affect the growth of co-cultured bacterial strains. The co-cultured bacterial cell counts in dual-species biofilms were not significantly different ($P > 0.05$) compared to their mono-species biofilm (Table S1). In *C. jejuni-S. enterica* and *C. jejuni-S. aureus* biofilms, the viable cell counts of *C. jejuni* were about 1 order of magnitude less than that of co-cultured bacterial strain. In *C. jejuni-P. aeruginosa* biofilm, the viable cell counts of *C. jejuni* were about 3 order of magnitude less than that of co-cultured bacterial strain. In general, *C. jejuni* was not the dominant strain compared to the co-cultured strains.

Under aerobic stress, *C. jejuni* F38011 cell counts in mono- and dual-species biofilms decreased over exposure time, but survival time and rate of decrease varied significantly (Table 1). *C. jejuni* cells in mono-species biofilm and *C. jejuni-P. aeruginosa* biofilm survived for the shortest time, with no culturable *C. jejuni* cells detected when the biofilms were exposed to aerobic stress at 4 days and 3 days, respectively. The initial *C. jejuni* cell counts in *C. jejuni-P. aeruginosa* biofilms were two orders of magnitude lower than that in mono-species *C. jejuni* biofilm, thus, the decreasing rate of *C. jejuni* cells in *C. jejuni-P. aeruginosa* biofilm was lower than that in mono-species biofilm. A large number of *C. jejuni* cells in the other two dual-species biofilms were still culturable at day 5, with the *C. jejuni* cell counts in *C. jejuni-S. enterica* and *C. jejuni-S. aureus* biofilms at 3.9 and 4.2 log CFU/cm^2, respectively. In contrast, the survival of non-*C. jejuni* strains was not affected by aerobic stress. Taken together, the cell counts of *S. enterica*, *S. aureus* and *P. aeruginosa* did not significantly decrease over exposure to aerobic stress.

3.2. Viability of C. jejuni F38011 cells in biofilms

The survival of *C. jejuni* F38011 sessile cells in biofilms under aerobic stress was further explored using confocal laser scanning microscopy (CLSM). When no *C. jejuni* cells were culturable in *C. jejuni* mono-species biofilm after four day of aerobic exposure, live cells could still be observed in live/dead staining images (Fig. 1a), suggesting that either the amount of live *C. jejuni* cells in mono-species biofilm were lower than the limit of detection of plating assay (2.7 log CFU/cm^2) or a large proportions of these live cells lost colony forming ability. We further observed that intense viable cell signals were aggregated at the bottom layer of biofilm, indicating survived *C. jejuni* cells tend to habit at the bottom of biofilm and away from the air-biofilm interface (Fig. 1b).

3.3. Formation level of C. jejuni biofilms

Both mono- and dual-species *C. jejuni* biofilms were cultivated under microaerobic conditions (N_2 85%, CO_2 10%, O_2 5%) at 37 °C for up to 72 h until maturation was reached. The level of biofilm formation at solid-liquid interface was determined using crystal violet staining assay (Fig. 2). Mono-species *C. jejuni* biofilm did not form well at the solid-liquid interface under static cultivation. In contrast, the formation level of all dual-species *C. jejuni* biofilms was significantly ($P < 0.05$) higher. Among these dual-species biofilms, a mixed culture of *C. jejuni* with *P. aeruginosa* had greatest biofilm formation, approximately 13.5 times higher than a mono-species *C. jejuni* biofilm (Fig. 2). *C. jejuni-S. enterica* mixture produced a biofilm mass 4 times greater than the mono-species

Table 1
Viable *C. jejuni* F38011 cell counts in mature biofilms with aerobic stress.

Time	Biofilms/viable cell counts (log CFU/cm^2)			
	C. jejuni	*C. jejuni* + *S. enterica*	*C. jejuni* + *S. aureus*	*C. jejuni* + *P. aeruginosa*
Mature (72-h cultivation, Day 0)	8.1 ± 0.1	7.8 ± 0.2	8.2 ± 0.1	5.9 ± 0.2
Day 1	7.4 ± 0.3	7.0 ± 0.3	7.2 ± 0.3	4.6 ± 0.2
Day 2	5.3 ± 0.3	5.9 ± 0.3	6.9 ± 0.7	3.9 ± 0.2
Day 3	4.9 ± 0.1	5.0 ± 0.3	5.2 ± 0.3	ND
Day 4	ND[a]	4.7 ± 0.1	4.8 ± 0.1	ND
Day 5	ND	3.9 ± 0.1	4.2 ± 0.1	ND

Day 1 to Day 5: exposure time of mature biofilm to aerobic environment.
[a] ND: non-detectable, the limit of detection is 2.7 log CFU/cm^2.

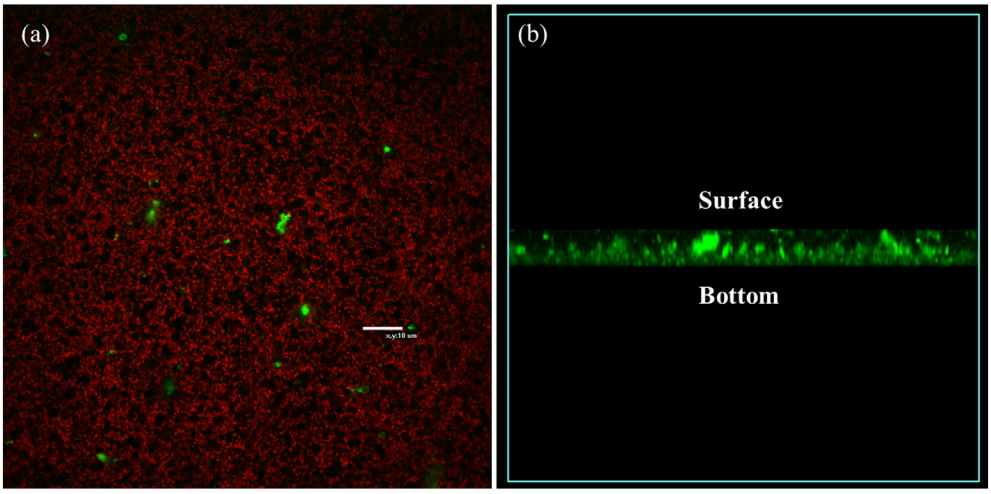

Fig. 1. Confocal laser scanning microscopy demonstrates the viability of *C. jejuni* F38011 sessile cells in mono-species biofilm under aerobic stress after 4 days. a) Viable and dead *C. jejuni* cells in mono-species biofilm showed in horizontal layout. b) Viable *C. jejuni* cells in mono-species biofilm showed in vertical layout. In this image, green color indicates live *C. jejuni* cells while red color indicates dead *C. jejuni* cells (n = 3). (For interpretation of the references to color in this figure legend, the reader is referred to the web version of this article.)

C. jejuni biofilm under the same cultivation condition. For dual-species biofilms, biofilm mass formation by *C. jejuni-P. aeruginosa* was significantly higher ($P < 0.05$) than *C. jejuni-S aureus* and *C. jejuni-S. enterica*. No significant difference was ($P > 0.05$) observed between *C. jejuni-S. aureus* and *C. jejuni-S. enterica* biofilms.

3.4. Contribution of *C. jejuni* to biofilm formation

C. jejuni share (CJS) index was calculated to estimate the effect of mixed bacterial culture (*i.e.*, *S. aureus*, *S. enterica* and *P. aeruginosa*) on biofilm formation ability of encased *C. jejuni* cells. By subtracting the biomass formed by non-*C. jejuni* strain in dual-species biofilm, the contribution from *C. jejuni* alone to dual-species biofilm mass could be roughly estimated. Subsequently, the contribution of *C. jejuni* to biofilm formation could be determined by comparing the amount of biofilm mass formed by *C. jejuni* in mono- and dual-species biofilms (formula shown in Section 2.6). The contribution of *C. jejuni* to biofilm formation was not affected by the presence of *S. aureus*, *P. aeruginosa*, or *S. enterica*, according to the CJS values calculated (Table 2).

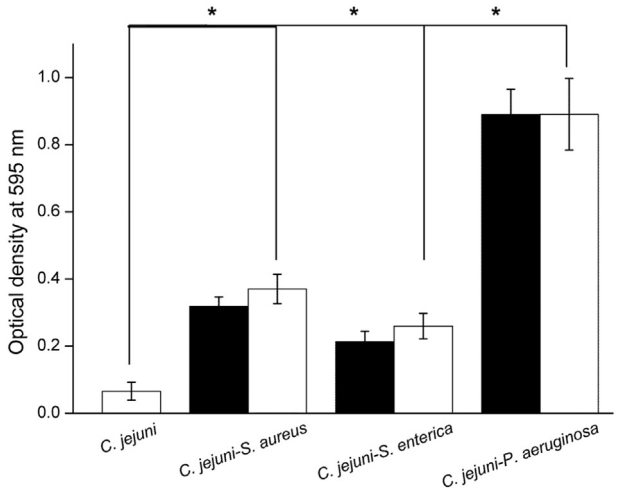

Fig. 2. Formation level of bacterial biofilms. (white column: *C. jejuni* containing biofilms; black column: non-*C. jejuni* containing biofilms). Asterisk denotes significant difference ($P < 0.05$) between mono-species *C. jejuni* biofilm and dual-species *C. jejuni* biofilms under the same inoculation concentration and cultivation conditions.

3.5. Chemical compositions of *C. jejuni* biofilms

Raman spectral patterns of mono- and dual-species *C. jejuni* biofilms were determined using confocal micro-Raman spectroscopy over a wavenumber region of 1800 to 400 cm^{-1}. A representative Raman spectrum of each biofilm was an average of 24 spectra collected from three independent experiments (Fig. 3). According to the previous studies of band assignments for bacteria and other biological systems (Lu et al., 2012a; Movasaghi et al., 2007), spectral regions depicting four important chemical components in biofilms are: 1800–1500 cm^{-1}: proteins, 1500–1200 cm^{-1}: fatty acids, 1200–900 cm^{-1}: polysaccharides, and 900–400 cm^{-1}: a unique fingerprinting region of mixed constituents.

C. jejuni-S. enterica biofilm shared a similar Raman spectral pattern to mono-species *C. jejuni* biofilm with the bands at 425, 578, 670, 780, 973, 997, 1100, 1336, 1445, and 1653 cm^{-1}, but at an enhanced signal intensity. Table 3(A)) summarizes the major Raman band assignments of mono- and dual-species *C. jejuni* biofilms, noting the spectral features of both EPS and encased cells within biofilms. Second derivative transformations were performed to magnify the minor variations in raw Raman spectra between mono-species *C. jejuni* biofilm and *C. jejuni-S. enterica* biofilm (Fig. S1). Distinct differences were observed at 425, 578, 780, 855, 997, and 1280 cm^{-1}, as summarized in Table 3(A)).

C. jejuni-S. aureus and *C. jejuni-P. aeruginosa* biofilms were significantly different in chemical compositions from each other and also from the mono-species *C. jejuni* biofilm, specifically at bands for lipids, proteins, and polysaccharides. Table 3(B)) summarizes the differences observed in spectral features for these biofilms.

Confocal micro-Raman spectroscopy was also applied to characterize non-*C. jejuni*-containing biofilms. Representative Raman spectra of each biofilm are shown in Fig. S2. Biofilms formed by non-*C. jejuni* strains (*i.e. S. enterica*, *S. aureus* and *P. aeruginosa*) shared similar Raman spectral pattern compared to the dual-species biofilm

Table 2
Contribution of *C. jejuni* F38011 cells to the formation of mono- and dual-species biofilms.

C. jejuni share (CJS) index in mono- and dual-species biofilms is summarized			
C. jejuni	*C. jejuni* + *S. enterica*	*C. jejuni* + *S. aureus*	*C. jejuni* + *P. aeruginosa*
1.00	1.07	0.99	0.97

The value is obtained as the ratio of biomass formed (per cell) by *C. jejuni* alone in dual-species biofilm to that formed (per cell) by *C. jejuni* in its mono-species biofilm (formula shown in Section 2.6).

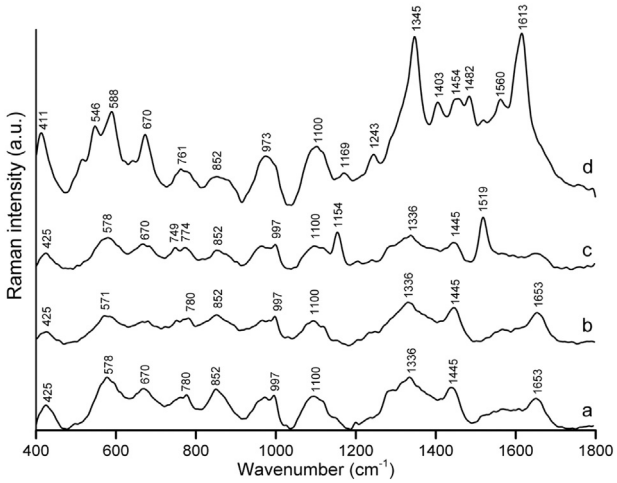

Fig. 3. Confocal Raman microspectroscopy characterizes the chemical compositions of mono- and dual-species *C. jejuni* biofilms: a) *C. jejuni*; b) *C. jejuni-S. enterica*; c) *C. jejuni-S. aureus*; d) *C. jejuni-P. aeruginosa.*

counterparts (*i.e. S. enterica* + *C. jejuni*, *S. aureus* + *C. jejuni*, and *P. aeruginosa* + *C. jejuni*), respectively. Only *P. aeruginosa* biofilm showed two distinct Raman bands at 516 and 1524 cm^{-1} (Table S3) that were not observed in the dual-species biofilm counterpart (*i.e. P. aeruginosa* + *C. jejuni*). In addition, the band intensities of Raman spectra of *S. enterica* and *S. aureus* biofilms were lower than their *C. jejuni*-containing dual-species biofilm counterparts (*i.e. S. enterica* + *C. jejuni* and *S. aureus* + *C. jejuni*). Raman band intensities were associated with the amount of chemical composition in biofilms, indicating that the removal of *C. jejuni* from mixed culture reduced biofilm mass formation. The result of Raman spectroscopic assay was also consistent to the result of biofilm mass formation determined by crystal violet staining assay. For *P. aeruginosa* biofilm, when *C. jejuni* cells were removed from the mixed culture, only the intensity of Raman band at 588 cm^{-1} (assigned to phospholipids) extensively decreased compared to *C. jejuni-P. aeruginosa* biofilm, indicating that *C. jejuni* contributed most of phospholipids to *C. jejuni-P. aeruginosa* biofilm.

PCA was employed to differentiate of mono- and dual-species *C. jejuni* biofilms based on Raman spectral patterns (Fig. S3). Each type of biofilm had distinctive features as signified by the formation of tight clusters with interclass distances for the biofilms from different species ranging from 4.63 to 13.02 based on *Mahalanobis* distance measurements computed between the centroids of groups. Clusters with interclass distance values higher than 3 are considered to be significantly different ($P < 0.05$) from each other (Lu et al., 2011a, 2011b).

Table 3(A)
. Raman band assignments for *C. jejuni* mono-species biofilm and *C. jejuni-S. enterica* biofilm.

Raman shift (cm^{-1})	Band assignment
425	Symmetric stretching vibration of phosphate
578	tryptophan/cytosine, guanine
670	ring breathing modes in DNA base
780	ring breathing of nucleotide
855	ring breathing modes in RNA base
973	C—C backbone of proteins
997	C—O vibration and C—C backbone of polysaccharides
1100	C—C vibration mode of amide III
1280	Backbone of nucleic acids and proteins
1336	CH_3CH_2 wagging of nucleic acids
1445	CH_3CH_2 banding mode of lipids and proteins
1653	amide I and C═C lipid stretch

Table 3(B)
. Unique Raman band assignments for *C. jejuni-S. aureus* and *C. jejuni-P. aeruginosa* biofilms[a].

Biofilms	Raman shift (cm^{-1})	Band assignment
C. jejuni-S. aureus	1519	C═C band stretch of polysaccharides
	1154	C—C stretching of proteins
	774	Symmetric breathing of proteins
	749	Symmetric breathing of lipids
C. jejuni-P. aeruginosa	1613	Tyrosine
	1560	Tryptophan
	1482	Ring breathing mode of nucleic acids
	1454	CH_3 bending of phospholipids
	1403	Methyl group in proteins
	1345	CH deformation of polysaccharides
	1243	Amide III
	1169	Tyrosine
	761	Ring breathing of tryptophan
	588	Symmetric stretching vibration of phospholipids
	546	Lipids
	411	Phospholipids

[a] Other band assignments are summarized in Table 3(A)).

3.6. Morphological and surface roughness profiles of *C. jejuni* biofilms

Surface morphological properties of mono- and dual-species *C. jejuni* biofilms were determined using AFM in contact mode and the representative topographic images are shown in Fig. 4. Twenty topographic images at random locations in three independent experiments were collected for each biofilm. Although AFM contact mode might result in surface rupture by friction, trace and retrace images closely fitted in the current study (data not shown), indicating that pressure from the AFM tip did not cause surface damage, and that the morphological properties and surface roughness parameters derived from AFM determinations were reliable. Deflection images provided detailed topographic information about the biofilm surface. Specifically, the surface of mono-species *C. jejuni* biofilm was loosely structured without an easily defined pattern as observed for the dual-species biofilms (Fig. 4a); in contrast, *C. jejuni* dual-species biofilms had tightly compact surface structures. Congested pits with size of 1 × 1 μm^2 with random arrangement were observed on the surface of *C. jejuni-S. enterica* (Fig. 4b) and *C. jejuni-P. aeruginosa* (Fig. 4d) biofilms while *C. jejuni-S. aureus* biofilm had a uniform surface structure with small shallow pits (Fig. 4c)

Topographic information for the non-*C. jejuni*-containing biofilms (*i.e. S. enterica*, *S. aureus* and *P. aeruginosa*) was also recorded using AFM (Fig. 4) (n = 20). The biofilms formed by *S. enterica*, *S. aureus* and *P. aeruginosa* alone had a relative compact structure. The surface pattern of biofilms formed by *P. aeruginosa* with or without *C. jejuni* was almost identical (Fig. 4d). In contrast, *S. enterica* and *S. aureus* biofilms showed differences with their dual-species biofilm counterparts (*i.e. S. enterica* + *C. jejuni* and *S. aureus* + *C. jejuni*) from the perspective of surface microstructure (Fig. 4b, c). Although a similar surface pattern (pits with size of 1 × 1 μm^2) to *C. jejuni-S. enterica* biofilm could be observed on *S. enterica* biofilm, the patterns were loosely organized. Compared to *C. jejuni- S. aureus* biofilm, *S. aureus* biofilm contained a greater number of bumps or protrusions on the surface, but small shallow pits spreading on *C. jejuni-S. aureus* biofilm could not be observed.

Root mean square (RMS) roughness indicated surface roughness of biofilms and this was calculated from height images (Fig. S4). RMS roughness value was 257.7 nm for *C. jejuni* mono-species biofilm, and for dual-species biofilms: 17.9 nm for *C. jejuni-S. enterica*, 30.7 nm for *C. jejuni-S. aureus*, and 27.4 nm for *C. jejuni-P. aeruginosa* (Fig. 5). The structural pattern of biofilms together with RMS roughness indicated that *C. jejuni* biofilms with an apparently loose structure have a rougher

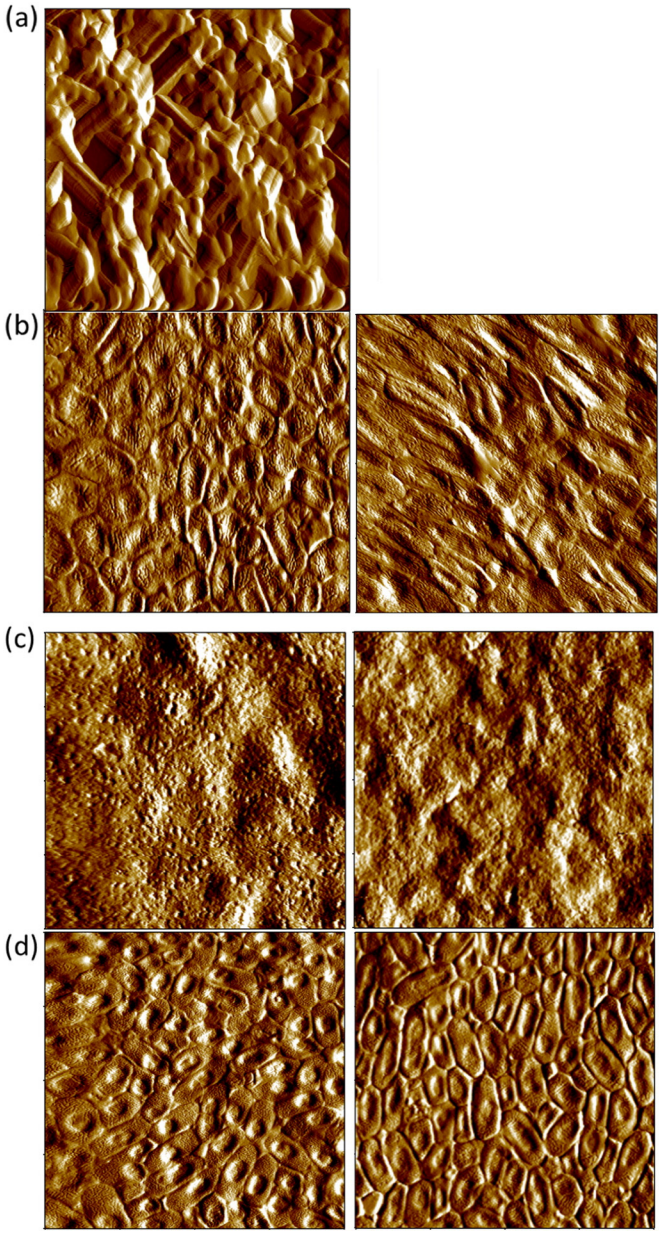

Fig. 4. Topographic deflection-retrace images of mono- and dual-species *C. jejuni* biofilms obtained by atomic force microscopy in contact mode within 8 μm × 8 μm area: a) *C. jejuni*; b) *C. jejuni-S. enterica*; c) *C. jejuni-S. aureus*; d) *C. jejuni-P. aeruginosa*. (left panels: *C. jejuni*-containing biofilms; right panels: non-*C. jejuni*-containing biofilms) (n = 20).

surface while the surface of tightly compact biofilms was much smoother. Three-dimensional images of surface roughness of mono- and dual-species *C. jejuni* biofilms are shown in Supplementary materials (Fig. S5) and highlighted the morphological variations of the biofilm surfaces.

The values of RMS roughness for non-*C. jejuni*-containing biofilms (*i.e. S. enterica*, *S. aureus* and *P. aeruginosa*) were 29.0 nm, 42.8 nm, and 30.2 nm, respectively (Fig. 5). Compared to the *C. jejuni*-containing dual-species biofilm counterparts, the values of RMS roughness for biofilms formed by *S. enterica* and *S. aureus* alone were significantly ($P < 0.05$) higher. There was a tendency for the RMS roughness for *P. aeruginosa* biofilm to be slightly enhanced compared to its dual-species biofilm counterpart, but no significant difference ($P > 0.05$) was observed. The structural pattern of biofilms together with RMS roughness indicated that *S. enterica* and *S. aureus* biofilms with loose structure have a rougher surface than their *C. jejuni*-containing dual-species biofilms.

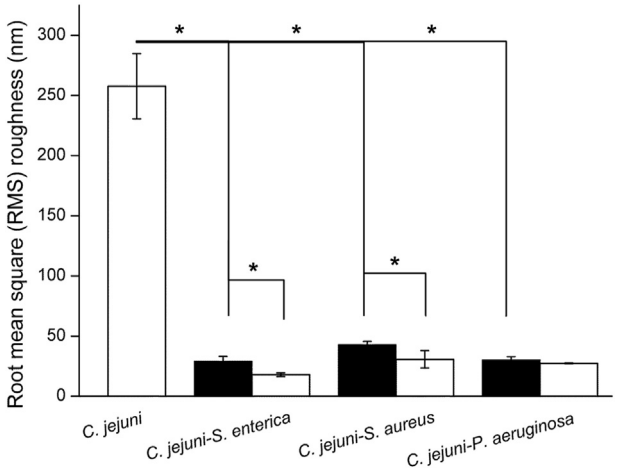

Fig. 5. Surface roughness of mono- and dual-species *C. jejuni* biofilms. (white column: *C. jejuni* containing biofilms; black column: non-*C. jejuni* containing biofilms). Asterisk denotes significant difference ($P < 0.05$).

No significant difference ($P > 0.05$) was observed from biofilms formed by *P. aeruginosa* with or without *C. jejuni*.

3.7. Surface wettability and free energy property of *C. jejuni* biofilms

The large and flat area of *C. jejuni* biofilms formed at solid-air interface facilitated the determination of surface wettability by contact angle measurement. Wettability using three reference liquids (*i.e.*, water, formamide and diiodomethane) with different surface energy properties was tested (Van Oss, 1993) and results summarized in Supplementary materials (Table S2). Water contact angle can be used as a qualitative parameter of biofilm surface hydrophobicity. When a water droplet is repelled and the contact angle is higher than 90°, the surface is hydrophobic. The higher the water contact angle is, the higher the hydrophobicity of the biofilm surface. In contrast, if a water droplet tends to spread on a surface and the contact angle is lower than 90° a surface is more hydrophilic. Representative images of contact angle formed on the surface of mono- and dual-species *C. jejuni* biofilms are shown in Supplementary materials (Fig. S6). Water droplets were quickly spread on the surface of mono-species biofilm, forming a contact angle of 13.2°. Dual-species biofilms were more repellent to water droplets with significantly higher ($P < 0.05$) contact angles than for mono-species biofilm, ranging from 19.6° to 21.8°. Taken together, water contact angle formed on all biofilms were lower than 90° (Table 4), indicating that *C. jejuni*-containing biofilms had hydrophilic surfaces and the hydrophilicity of mono-species biofilms was higher than dual-species biofilms. The contact angle kept increasing when less polar liquids were applied, although with lower total surface energy. Specifically, contact angles of formamide ranged from 19.7° to 28.3° for *C. jejuni* biofilms; biofilms tended to repel the apolar diiodomethane

Table 4
Contact angle measurement of mono- and dual-species *C. jejuni* biofilms using sessile drop technique.

Culture	Contact angle		
	Water	Formamide	Diiodomethane
C. jejuni	13.2° ± 2.2°	19.7° ± 2.7°	82.6° ± 4.2°
C. jejuni + *S. enterica*	20.5° ± 2.4°*	25.0° ± 2.5°*	65.7° ± 3.4°*
S. enterica	16.5° ± 3.2°	23.7° ± 2.6°	71.5° ± 5.1°
C. jejuni + *S. aureus*	19.6° ± 1.8°*	22.8° ± 2.2°*	66.6° ± 2.9°*
S. aureus	19.2° ± 2.4°	20.1° ± 3.7°	74.5° ± 2.4°
C. jejuni + *P. aeruginosa*	21.8° ± 2.7°*	28.3° ± 2.8°*	62.4° ± 1.9°*
P. aeruginosa	21.6° ± 2.8°	27.1° ± 4.2°	65.4° ± 2.8°

* Significant difference ($P < 0.05$) was observed between mono-species *C. jejuni* biofilm and dual-species *C. jejuni* biofilms.

The contact angle measurement was also applied on non-*C. jejuni*-containing (*i.e. S. enterica*, *S. aureus* and *P. aeruginosa*) biofilms. The water contact angle formed on non-*C. jejuni*-containing biofilms was lower than the *C. jejuni*-containing biofilm counterparts, ranging from 16.5° to 21.6° (Table 4). This indicated that the hydrophilicity of non-*C. jejuni*-containing biofilms was higher than the *C. jejuni*-containing dual-species biofilm counterparts. The contact angle on non-*C. jejuni*-containing biofilms with other two reference liquids was also different from that of the *C. jejuni*-containing dual-species biofilm counterparts. Specifically, contact angles of formamide on non-*C. jejuni*-containing biofilms were lower (ranging from 20.1° to 27.1°) while diiodomethane was repelled on non-*C. jejuni*-containing biofilms, with contact angles ranging from 65.4° to 74.5°.

Surface energy can be calculated from contact angle measurement using Young-Dupré equation (Table 5). Compared to mono-species *C. jejuni* biofilm, the total surface energy was relatively lower in the dual-species biofilms. In addition, apolar component (Lifshitz-Van der Waals) and polar component (Lewis acid-base) of the surface energy of mono- and dual-species *C. jejuni* biofilms varied extensively. Specifically, the apolar component of surface energy in dual-species biofilms ranged from 24.7 to 27.1 mJ/m^2, which was significantly higher ($P < 0.05$) than that of mono-species biofilm (*i.e.*, 16.1 mJ/m^2). The mono-species biofilm repelled apolar liquid (*i.e.*, diiodomethane) more than dual-species biofilms did, with a greater polar component of surface energy, resulting in greater wetting by polar liquids (*i.e.*, water and formamide).

For non-*C. jejuni*-containing biofilms, the total surface energy of *S. aureus* and *P. aeruginosa* biofilms was higher than their *C. jejuni*-containing dual-species biofilm counterparts, but *S. enterica* biofilm had a lower total surface energy compared to *C. jejuni-S. enterica* biofilm. In addition, the apolar component of surface energy in non-*C. jejuni*-containing biofilms was lower than that of *C. jejuni*-containing dual-species biofilm counterparts, ranging from 20.4 to 25.5 mJ/m^2. The polar component of surface energy was increased when biofilms were formed without *C. jejuni*, ranging from 28.5 to 39.0 mJ/m^2.

3.8. Water-holding capability of C. jejuni biofilms

Water holding capability of bacterial biofilms is critical because it affects hydration of biofilm systems and consequently the survival of sessile bacterial cells. Water content of mono- and dual-species *C. jejuni* biofilms was determined using FT-IR spectroscopy (Fig. S7). Water has a distinct IR absorbance band at 3350 cm^{-1}, the O—H stretch, and intensity for all *C. jejuni* biofilms was initially similar (Fig. 6) and ~0.3 or the same as pure water. This indicated substantial free water was present in *C. jejuni* biofilms, but as the mono-species *C. jejuni* biofilm was exposed to the atmosphere, band intensity sharply dropped to 0.04 within 25 min and then remained stable. In contrast, dual-species *C. jejuni* biofilms had higher water holding capability and the magnitude of the absorbance band for water declined more slowly with the band intensities after 25-min desiccation, at 0.25 for *C. jejuni-S. enterica*, 0.18 for *C. jejuni-S. aureus* and 0.20 *C. jejuni-P. aeruginosa* biofilms, respectively

No significant difference ($P > 0.05$) was observed for water holding capability of biofilms formed by *P. aeruginosa* with or without *C. jejuni*. In contrast, for both *S. enterica* and *S. aureus* biofilms, water content started to decrease sharply after desiccation from 10-min air exposure, and was significantly ($P < 0.05$) lower than that in *C. jejuni*-containing dual-species biofilm counterparts (*S. enterica* + *C. jejuni* and *S. aureus* + *C. jejuni*) after 25-min air exposure (Fig. 6).

4. Discussion

C. jejuni could form biofilms at different material surfaces, including plastics (Asakura et al., 2007; Reeser et al., 2007; Trachoo et al., 2002), stainless steel (Gunther and Chen, 2009; Hanning et al., 2008; Sanders et al., 2007), and glass (Dykes et al., 2003; Kalmokoff et al., 2006). Biofilm formation capability varied among different *C. jejuni* strains. For example, *C. jejuni* RM 1221 was unable to form a biofilm even in a well-controlled laboratory environment; in contrast, *C. jejuni* NCTC 11168 could form a relatively high level of biofilm under the same condition (Brown et al., 2014). *C. jejuni* F38011 used in this study is a human clinical isolate. This strain could only form a thin biofilm at both solid-air interface and solid-liquid interface, which was confirmed by crystal violet staining assay and Raman spectroscopy (Fig. 2 and Fig. 3). The biofilm formation capability of *C. jejuni* F38011 is similar to other *C. jejuni* strains reported in the previous studies (Gunther and Chen, 2009; Teh et al., 2010); therefore the result derived from this strain could be representative.

Environmental conditions are critical to *C. jejuni* biofilm formation. Aerobic condition has been validated to accelerate *C. jejuni* biofilm formation at the air-solid interface (Reuter et al., 2010). High flow rate with corresponding high shear force would increase structural porosity of *C. jejuni* biofilm formed at liquid-solid interface (Ica et al., 2012). A photonic-based microfluidic platform was recently developed to elucidate the impact of flow condition on biofilm formation (Feng et al., 2015). In the current study, these factors are not included because it will complicate the evaluation of dual-species culture influence on biofilm formation and the survival state of encased *C. jejuni*.

In the current study, sessile *C. jejuni* cells in mono-species biofilm could not maintain a culturable state over 4 days under aerobic stress (Table 1). However, CLSM result demonstrated that a large amount of cells at the bottom of biofilm were still alive (Fig. 1a and b). According to previous studies, *C. jejuni* may lose cultivability and enter the "viable but non-culturable" (VBNC) state because of sensing unfavorable conditions, such as aerobic stress, desiccation, and starvation (Lázaro et al., 1999; Oliver, 2005; Tholozan et al., 1999). *C. jejuni* cells at the bottom of biofilm may share a viable similarity to VBNC cell and had an enhanced resistance to the aerobic stress.

Multispecies *C. jejuni* biofilms could be developed either by a premixed culture (Ica et al., 2012) or attachment of *C. jejuni* floating cells to a pre-established biofilm by other bacteria (Buswell et al., 1998; Hanning et al., 2008; Sanders et al., 2007; Trachoo et al., 2002). Sanders and coauthors reported that *C. jejuni* cells had prolonged survival through attachment to the pre-existing biofilms in a watering system (Sanders et al., 2007). In another study, the enhanced survival of *C. jejuni* cells was reported to be twice as long in the pre-established biofilms by microbes in aquatic environment (Buswell et al., 1998). Similar observation was also reported for secondary attachment of *C. jejuni* to the pre-

Table 5
Surface energy and distribution of energy components of mono- and dual-species *C. jejuni* biofilms.

Culture	Total surface energy (mJ/m^2)	Surface energy component distribution (mJ/m^2)	
		Lifshitz-Van der Waals (apolar component)	Lewis acid-base (polar component)
C. jejuni	62.9	16.1	46.7
C. jejuni + *S. enterica*	55.0	25.2	29.8
S. enterica	57.5	22.0	35.4
C. jejuni + *S. aureus*	56.2	24.7	31.5
S. aureus	59.4	20.4	39.0
C. jejuni + *P. aeruginosa*	52.5	27.1	25.4
P. aeruginosa	53.9	25.5	28.5

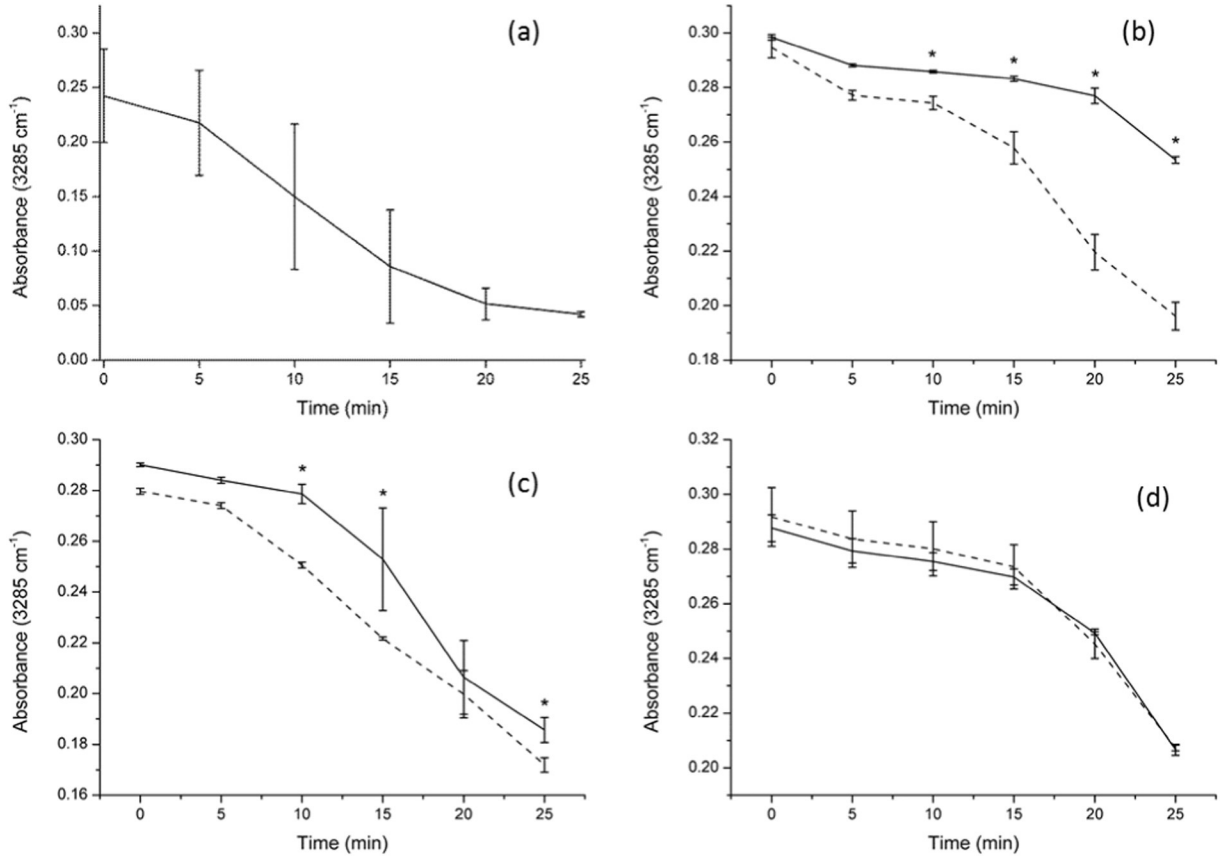

Fig. 6. Water holding capability of mono- and dual-species *C. jejuni* biofilms. Water content of biofilms was determined by Fourier transform infrared spectroscopy, as indicated by the featured absorbance band at 3285 cm^{-1}: a) *C. jejuni*, b) *C. jejuni-S. enterica*, c) *C. jejuni-S. aureus*; d) *C. jejuni-P. aeruginosa*. (solid line: *C. jejuni*-containing biofilms, dash line: non-*C. jejuni*-containing biofilms). Asterisk denotes significant difference ($P < 0.05$).

established biofilms formed either by *Pseudomonas* (Trachoo et al., 2002) or bacteria isolated from poultry farms (Hanning et al., 2008). Our current study demonstrated that *C. jejuni* could form a biofilm with different bacteria, but did not take domination position in dual-species biofilms (Table 1 and Table S1). Compared to mono-species *C. jejuni* biofilm, the formation level of dual-species *C. jejuni* biofilms was significantly higher (Fig. 2 and Fig. 3). However, according to the CJS index values (Table 2), the contribution of *C. jejuni* cells to dual-species biofilms was similar to that of mono-species biofilm (Fig. 2), indicating that mixed culture had no effect on biofilm formation capability of *C. jejuni*. Compared to mono-species *C. jejuni* biofilm, culturable state of *C. jejuni* cells could be maintained for a longer period in most dual-species biofilms under aerobic stress (Table 1). Overall, mono-species *C. jejuni* produced similar amount of EPS in both mono- and dual-species biofilms, but received more protection in dual-species biofilms than that in mono-species biofilm.

Although *C. jejuni-P. aeruginosa* culture produced a biofilm with the highest EPS content, the culturable cell count and survival time of *C. jejuni* in this biofilm were the lowest (Table 1). Gram-negative bacteria secret outer membrane vesicles containing a range of enzymes and virulence metabolites that could inhibit competing organisms in biofilms (Flemming and Wingender, 2010). *P. aeruginosa* membrane vesicles contained various compounds (*e.g.*, B-band lipopolysaccharide with hemolysin, phospholipase C and alkaline phosphatase) that can inhibit the growth of other bacteria (Kadurugamuwa and Beveridge, 1995). Thus, *C. jejuni* and *P. aeruginosa* were in a competitive relationship during biofilm formation. *P. aeruginosa* multiplied rapidly and limited the growth space for *C. jejuni* at the initial stage of biofilm formation. Toxic secondary metabolites (*e.g.*, hemolysin, phospholipase C and alkaline phosphatase) secreted by *P. aeruginosa* further negatively affect the survival of *C. jejuni* in the biofilm.

Biofilms can protect encased cells from aerobic stress, but the mechanism of stress resistance is not clear. Three explanations can be provided: biofilm chemical components react with stress inducer (Allison and Matthews, 1992), biofilm chemical components serve as nutrient reservoirs for sessile cells (Decho et al., 2005), and biofilm structure inhibits stress inducer penetration (Ica et al., 2012). Biofilms are mainly composed of proteins and polysaccharides with less lipids and nucleic acids (Flemming and Wingender, 2010). Hence, the chemical components of a biofilm are closely associated with its stress resistance. In the previous studies, Raman spectroscopy has been validated to determine EPS components of mono-species *C. jejuni* biofilm (Lu et al., 2012a; Lu et al., 2012b). In this study, Raman spectroscopy in a confocal mode was applied to dual-species biofilms. Dual-species biofilms had a different chemical composition than mono-species biofilm based upon different Raman spectral features (Fig. 3). Distinctive Raman bands absent in *C. jejuni* mono-species biofilm confirmed that additional chemical components were clearly present in dual-species biofilms (Table 3(B))). Specifically, Raman bands at 1519 and 1345 cm^{-1} are derived from polysaccharides and these were significant components in *C. jejuni-S. aureus* and *C. jejuni-P. aeruginosa* biofilms, but not distinctive in mono-species *C. jejuni* biofilm. As indicated by Raman band intensity, dual-species biofilms contained more content of organic substances, which was in consistent to the results of biofilm staining assay (Fig. 2). In addition, Raman spectral pattern of non-*C. jejuni*-containing biofilms was highly similar to that of *C. jejuni*-containing dual-species biofilm counterparts, indicating that additional Raman bands not present in mono-species *C. jejuni* biofilm were mainly derived from non-*C. jejuni* strains. However, Raman band intensity of non-*C. jejuni*-containing biofilms was generally lower than that of *C. jejuni*-containing dual-species biofilm counterparts, indicating that *C. jejuni* also produce EPS components and contribute to dual-species biofilm development

which was in consistent to the results of biofilm staining assay (Fig. 2) and CJS index calculation (Table 2).

The relationship between chemical compositions of the biofilm and its structural properties were investigated by previous studies. For example, a non-cellular protein was identified to be a prerequisite for granule formation and related to biofilm stability (McSwain et al., 2005). In the current study, changes in biofilm structure were partially correlated to changes in chemical composition. AFM topographic images (Fig. 4, Fig. S4 and Fig. 5) showed that dual-species biofilms had a compact structure with a smoother surface than mono-species *C. jejuni* biofilm, while Raman intensity of polysaccharides and proteins in dual-species biofilms was higher than that in mono-species *C. jejuni* biofilm (Fig. 3), indicating that these macromolecules contribute more to the structural properties of dual-species biofilms than other components (*e.g.*, lipids). Introduction of non-*C. jejuni* strains into biofilm enhanced the concentration and diversity of biofilm chemical compositions and these constituents may serve as a glue to fill the space of multicellular structure of biofilm, contributing to biofilm stability.

Physical properties of *C. jejuni* biofilms, including water holding capability, surface wettability and surface free energy, were also changed along with the introduction of non-*C. jejuni* strains. Dual-species biofilms retained water for a longer time than mono-species *C. jejuni* biofilm (Fig. 6). Raman spectroscopic result showed that the introduction of non-*C. jejuni* elevated the content of hydrophilic substances, specifically polysaccharides and proteins in dual-species biofilms (Fig. 3), which are responsible for enhanced water holding capability. Thus, water holding capability in dual-species biofilms was associated with a higher content of polysaccharides and proteins that were mainly derived from non-*C. jejuni* strains.

Introduction of non-*C. jejuni* strains slightly affect the wetting properties of biofilms, resulting in a decrease in apolar liquid contact angle but an increase in polar liquid contact angle (Table 4). Within a biofilm, lipid is the major structural constituent that is associated with wetting properties. As shown in Raman spectroscopic analysis, lipid content increased by introducing non-*C. jejuni* strains in dual-species *C. jejuni* biofilms (Fig. 3). The increase in lipid content might lead to an increased ratio of apolar component (Lifshitz-*V*an der Waals)/polar component (Lewis acid-base) of surface energy, which is completely consistent to our current observation in this study (Table 5).

In conclusion, this study demonstrated that mono-species *C. jejuni* F38011 culture could form a thin biofilm, but only maintained the culturable state of *C. jejuni* cells for a short time (96 h). Biofilm biomass formed by mixed cultures of *S. enterica*, *S. aureus* and *P. aeruginosa* with *C. jejuni* was much higher and the variations in chemical, physical and morphological profiles could be observed between these and mono-species *C. jejuni* biofilm. The dual-species biofilms (1) contained a higher concentration EPS with a more complex chemical compositions; (2) were more compact with smoother surface; (3) were less hydrophilic but with a higher ratio of apolar component/polar component of surface energy to maintain a high water content for a longer time. These features were mainly derived from the non-*C. jejuni* strains (*i.e.*, *S. enterica*, *S. aureus* and *P. aeruginosa*) in the dual-species culture, and allowed the encased *C. jejuni* F38011 cells in dual-species biofilms to survive under aerobic stress for a longer time.

Acknowledgements

Financial support to X.L. in the form of a Discovery Grant from the National Sciences and Engineering Research Council of Canada (NSERC RGPIN-2014-05487) is gratefully acknowledged. J.F. received a 4-year Ph.D. fellowship from the China Scholarship Council.

Appendix A. Supplementary data

Supplementary data to this article can be found online at http://dx.doi.org/10.1016/j.ijfoodmicro.2016.09.008.

References

Allison, D., Matthews, M., 1992. Effect of polysaccharide interactions on antibiotic susceptibility of *Pseudomonas aeruginosa*. J. Appl. Microbiol. 73, 484–488.
Allison, D., Brown, M., Evans, D., Gilbert, P., 1990. Surface hydrophobicity and dispersal of *Pseudomonas aeruginosa* from biofilms. FEMS Microbiol. Lett. 71, 101–104.
Asakura, H., Yamasaki, M., Yamamoto, S., Igimi, S., 2007. Deletion of peb4 gene impairs cell adhesion and biofilm formation in *Campylobacter jejuni*. FEMS Microbiol. Lett. 275, 278–285.
Beech, I.B., Smith, J.R., Steele, A.A., Penegar, I., Campbell, S.A., 2002. The use of atomic force microscopy for studying interactions of bacterial biofilms with surfaces. Colloids Surf. B: Biointerfaces 23, 231–247.
Beyenal, H., Donovan, C., Lewandowski, Z., Harkin, G., 2004. Three-dimensional biofilm structure quantification. J. Microbiol. Methods 59, 395–413.
Bove, P., Capozzi, V., Garofalo, C., Rieu, A., Spano, G., Fiocco, D., 2012. Inactivation of the *ftsH* gene of *Lactobacillus plantarum* WCFS1: Effects on growth, stress tolerance, cell surface properties and biofilm formation. Microbiol. Res. 167, 187–193.
Briandet, R., Herry, J.-M., Bellon-Fontaine, M.-N., 2001. Determination of the van der Waals, electron donor and electron acceptor surface tension components of static gram-positive microbial biofilms. Colloids Surf. B: Biointerfaces 21, 299–310.
Brown, H.L., Reuter, M., Salt, L.J., Cross, K.L., Betts, R.P., van Vliet, A.H., 2014. Chicken juice enhances surface attachment and biofilm formation of *Campylobacter jejuni*. Appl. Environ. Microbiol. 80, 7053–7060.
Buswell, C.M., Herlihy, Y.M., Lawrence, L.M., McGuiggan, J.T., Marsh, P.D., Keevil, C.W., Leach, S.A., 1998. Extended survival and persistence of *Campylobacter spp.* in water and aquatic biofilms and their detection by immunofluorescent-antibody and-rRNA staining. Appl. Environ. Microbiol. 64, 733–741.
Davies, D., 2003. Understanding biofilm resistance to antibacterial agents. Nat. Rev. Drug Discov. 2, 114–122.
Decho, A.W., Visscher, P.T., Reid, R.P., 2005. Production and cycling of natural microbial exopolymers (EPS) within a marine stromatolite. Palaeogeogr. Palaeoclimatol. Palaeoecol. 219, 71–86.
Donlan, R.M., Costerton, J.W., 2002. Biofilms: survival mechanisms of clinically relevant microorganisms. Clin. Microbiol. Rev. 15, 167–193.
Dykes, G., Sampathkumar, B., Korber, D., 2003. Planktonic or biofilm growth affects survival, hydrophobicity and protein expression patterns of a pathogenic *Campylobacter jejuni* strain. Int. J. Food Microbiol. 89, 1–10.
Feng, S., Eucker, T.P., Holly, M.K., Konkel, M.E., Lu, X., Wang, S., 2014. Investigating the responses of *Cronobacter sakazakii* to garlic-drived organosulfur compounds: a systematic study of pathogenic-bacterium injury by use of high-throughput whole-transcriptome sequencing and confocal micro-Raman spectroscopy. Appl. Environ. Microbiol. 80, 959–971.
Feng, J., de la Fuente-Núñez, C., Trimble, M.J., Xu, J., Hancock, R.E., Lu, X., 2015. An in situ Raman spectroscopy-based microfluidic "lab-on-a-chip" platform for non-destructive and continuous characterization of *Pseudomonas aeruginosa* biofilms. Chem. Commun. 51, 8966–8969.
Flemming, H.-C., Wingender, J., 2010. The biofilm matrix. Nat. Rev. Microbiol. 8, 623–633.
Gunther, N.W., Chen, C.-Y., 2009. The biofilm forming potential of bacterial species in the genus Campylobacter. Food Microbiol. 26, 44–51.
Hanning, I., Jarquin, R., Slavik, M., 2008. *Campylobacter jejuni* as a secondary colonizer of poultry biofilms. J. Appl. Microbiol. 105, 1199–1208.
Hermans, D., Van Deun, K., Martel, A., Van Immerseel, F., Messens, W., Heyndrickx, M., Haesebrouck, F., Pasmans, F., 2011. Colonization factors of *Campylobacter jejuni* in the chicken gut. Vet. Res. 42, 10.1186.
Ica, T., Caner, V., Istanbullu, O., Nguyen, H.D., Ahmed, B., Call, D.R., Beyenal, H., 2012. Characterization of mono-and mixed-culture *Campylobacter jejuni* biofilms. Appl. Environ. Microbiol. 78, 1033–1038.
Ivanov, I.E., Kintz, E.N., Porter, L.A., Goldberg, J.B., Burnham, N.A., Camesano, T.A., 2011. Relating the physical properties of *Pseudomonas aeruginosa* lipopolysaccharides to virulence by atomic force microscopy. J. Bacteriol. 193, 1259–1266.
Ivleva, N.P., Wagner, M., Horn, H., Niessner, R., Haisch, C., 2008. In situ surface-enhanced Raman scattering analysis of biofilm. Anal. Chem. 80, 8538–8544.
Ivleva, N.P., Wagner, M., Szkola, A., Horn, H., Niessner, R., Haisch, C., 2010. Label-free in situ SERS imaging of biofilms. J. Phys. Chem. B 114, 10184–10194.
Joshua, G.P., Guthrie-Irons, C., Karlyshev, A., Wren, B., 2006. Biofilm formation in *Campylobacter jejuni*. Microbiology 152, 387–396.
Kadurugamuwa, J.L., Beveridge, T.J., 1995. Virulence factors are released from *Pseudomonas aeruginosa* in association with membrane vesicles during normal growth and exposure to gentamicin: a novel mechanism of enzyme secretion. J. Bacteriol. 177, 3998–4008.
Kalmokoff, M., Lanthier, P., Tremblay, T.-L., Foss, M., Lau, P.C., Sanders, G., Austin, J., Kelly, J., Szymanski, C.M., 2006. Proteomic analysis of *Campylobacter jejuni* 11168 biofilms reveals a role for the motility complex in biofilm formation. J. Bacteriol. 188, 4312–4320.
Kumar, C.G., Anand, S., 1998. Significance of microbial biofilms in food industry: a review. Int. J. Food Microbiol. 42, 9–27.
La Storia, A., Ercolini, D., Marinello, F., Di Pasqua, R., Villani, F., Mauriello, G., 2011. Atomic force microscopy analysis shows surface structure changes in carvacrol-treated bacterial cells. Res. Microbiol. 162, 164–172.
Lamour, G., Hamraoui, A., Buvailo, A., Xing, Y., Keuleyan, S., Prakash, V., Eftekhari-Bafrooei, A., Borguet, E., 2010. Contact angle measurements using a simplified experimental setup. J. Chem. Educ. 87, 1403–1407.
Lázaro, B., Cárcamo, J., Audícana, A., Perales, I., Fernández-Astorga, A., 1999. Viability and DNA maintenance in nonculturable spiral *Campylobacter jejuni* cells after long-term exposure to low temperatures. Appl. Environ. Microbiol. 65, 4677–4681.

Li, B., Logan, B.E., 2004. Bacterial adhesion to glass and metal-oxide surfaces. Colloids Surf. B: Biointerfaces 36, 81–90.
Lim, J., Cui, Y., Oh, Y.J., Park, J.R., Jo, W., Cho, Y.-H., Park, S., 2011. Studying the effect of alginate overproduction on *Pseudomonas aeruginosa* biofilm by atomic force microscopy. J. Nanosci. Nanotechnol. 11, 5676–5681.
Lu, X., Wang, J., Al-Qadiri, H.M., Ross, C.F., Powers, J.R., Tang, J., Rasco, B.A., 2011a. Determination of total phenolic content and antioxidant capacity of onion (*Allium cepa*) and shallot (*Allium oschaninii*) using infrared spectroscopy. Food Chem. 129, 637–644.
Lu, X., Rasco, B.A., Kang, D.H., Jabal, J.M., Aston, D.E., Konkel, M.E., 2011b. Infrared and Raman spectroscopic studies of the antimicrobial effects of garlic concentrates and diallyl constituents on foodborne pathogens. Anal. Chem. 83, 4137–4146.
Lu, X., Samuelson, D.R., Rasco, B.A., Konkel, M.E., 2012a. Antimicrobial effect of diallyl sulphide on *Campylobacter jejuni* biofilms. J. Antimicrob. Chemother. 67, 1915–1926.
Lu, X., Weakley, A.T., Aston, D.E., Rasco, B.A., Wang, S., Konkel, M.E., 2012b. Examination of nanoparticle inactivation of *Campylobacter jejuni* biofilms using infrared and Raman spectroscopies. J. Appl. Microbiol. 113, 952–963.
Lu, X., Samuelson, D.R., Xu, Y., Zhang, H., Wang, S., Rasco, B.A., Xu, J., Konkel, M.E., 2013. Detecting and tracking nosocomial methicillin-resistant *Staphylococcus aureus* using a microfluidic SERS biosensor. Anal. Chem. 85, 2320–2327.
McSwain, B., Irvine, R., Hausner, M., Wilderer, P., 2005. Composition and distribution of extracellular polymeric substances in aerobic flocs and granular sludge. Appl. Environ. Microbiol. 71, 1051–1057.
Mirvakili, M.N., Hatzikiriakos, S.G., Englezos, P., 2013. Superhydrophobic lignocellulosic wood fiber/mineral networks. ACS Appl. Mater. Interfaces 5, 9057–9066.
Movasaghi, Z., Rehman, S., Rehman, I.U., 2007. Raman spectroscopy of biological tissues. Appl. Spectrosc. Rev. 42, 493–541.
Naves, P., del Prado, G., Huelves, L., Gracia, M., Ruiz, V., Blanco, J., Dahbi, G., Blanco, M., del Carmen Ponte, M., Soriano, F., 2008. Correlation between virulence factors and *in vitro* biofilm formation by *Escherichia coli* strains. Microb. Pathog. 45, 86–91.
Neal-McKinney, J.M., Lu, X., Duong, T., Larson, C.L., Call, D.R., Shah, D.H., Konkel, M.E., 2012. Production of organic acids by probiotic *Lactobacilli* can be used to reduce pathogen load in poultry. PLoS One 7, e43928.
Newell, D., Fearnley, C., 2003. Sources of *Campylobacter* colonization in broiler chickens. Appl. Environ. Microbiol. 69, 4343–4351.
Ng, J., Kidd, S.P., 2013. The concentration of intracellular nickel in *Haemophilus influenzae* is linked to its surface properties and cell–cell aggregation and biofilm formation. Int. J. Med. Microbiol. 303, 150–157.
Oliver, J.D., 2005. The viable but nonculturable state in bacteria. J. Microbiol. 43, 93–100.
Oyarzabal, O.A., Macklin, K.S., Barbaree, J.M., Miller, R.S., 2005. Evaluation of agar plates for direct enumeration of *Campylobacter spp.* from poultry carcass rinses. Appl. Environ. Microbiol. 71, 3351–3354.
Reeser, R.J., Medler, R.T., Billington, S.J., Jost, B.H., Joens, L.A., 2007. Characterization of *Campylobacter jejuni* biofilms under defined growth conditions. Appl. Environ. Microbiol. 73, 1908–1913.
Reuter, M., Mallett, A., Pearson, B.M., van Vliet, A.H., 2010. Biofilm formation by *Campylobacter jejuni* is increased under aerobic conditions. Appl. Environ. Microbiol. 76, 2122–2128.
Roberson, E.B., Firestone, M.K., 1992. Relationship between desiccation and exopolysaccharide production in a soil *Pseudomonas sp*. Appl. Environ. Microbiol. 58, 1284–1291.
Sanders, S.Q., Boothe, D.H., Frank, J.F., Arnold, J.W., 2007. Culture and detection of *Campylobacter jejuni* within mixed microbial populations of biofilms on stainless steel. J. Food Prot. 70, 1379–1385.
Scheuring, S., Dufrêne, Y.F., 2010. Atomic force microscopy: probing the spatial organization, interactions and elasticity of microbial cell envelopes at molecular resolution. Mol. Microbiol. 75, 1327–1336.
Siringan, P., Connerton, P.L., Payne, R.J., Connerton, I.F., 2011. Bacteriophage-mediated dispersal of *Campylobacter jejuni* biofilms. Appl. Environ. Microbiol. 77, 3320–3326.
Syamaladevi, R.M., Lu, X., Sablani, S.S., Insan, S.K., Adhikari, A., Killinger, K., Rasco, B., Dhingra, A., Bandyopadhyay, A., Annapure, U., 2013. Inactivation of *Escherichia coli* population on fruit surfaces using ultraviolet-C light: influence of fruit surface characteristics. Food Bioprocess Technol. 6, 2959–2973.
Tamaru, Y., Takani, Y., Yoshida, T., Sakamoto, T., 2005. Crucial role of extracellular polysaccharides in desiccation and freezing tolerance in the terrestrial cyanobacterium *Nostoc commune*. Appl. Environ. Microbiol. 71, 7327–7333.
Teh, K.H., Flint, S., French, N., 2010. Biofilm formation by *Campylobacter jejuni* in controlled mixed-microbial populations. Int. J. Food Microbiol. 143, 118–124.
Teh, A.H.T., Lee, S.M., Dykes, G.A., 2014. Does *Campylobacter jejuni* form biofilms in food-related environments? Appl. Environ. Microbiol. 80, 5154–5160.
Tholozan, J., Cappelier, J., Tissier, J., Delattre, G., Federighi, M., 1999. Physiological characterization of viable-but-nonculturable *Campylobacter jejuni* cells. Appl. Environ. Microbiol. 65, 1110–1116.
Trachoo, N., Frank, J., Stern, N., 2002. Survival of *Campylobacter jejuni* in biofilms isolated from chicken houses. J. Food Prot. 65, 1110–1116.
Van Oss, C., 1993. Acid—base interfacial interactions in aqueous media. Colloids Surf. A Physicochem. Eng. Asp. 78, 1–49.
van Oss, C.J., 2002. Use of the combined Lifshitz–van der Waals and Lewis acid–base approaches in determining the apolar and polar contributions to surface and interfacial tensions and free energies. J. Adhes. Sci. Technol. 16, 669–677.
Young, K.T., Davis, L.M., DiRita, V.J., 2007. *Campylobacter jejuni*: molecular biology and pathogenesis. Nat. Rev. Microbiol. 5, 665–679.